Date: Jan 6, 2017

EIC Detector R&D Progress Report

Project ID: eRD6
Project Name: Tracking and PID detector R&D towards an EIC detector
Period Reported: from July 2016 to December 2016
Project Leader:
Brookhaven National Lab: Craig Woody
Florida Tech: Marcus Hohlmann
INFN Trieste: Silvia Dalla Torre
Stony Brook University: Klaus Dehmelt, Thomas Hemmick
University of Virginia: Kondo Gnanvo, Nilanga Liyanage
Yale University: Richard Majka, Nikolai Smirnov

Contact Person: Klaus Dehmelt

Project members:
Brookhaven National Lab: B. Azmoun, M. L. Purschke, C. Woody
Brookhaven National Lab - Medium energy group: A. Kiselev
Florida Tech: M. Hohlmann, A. Zhang
Stony Brook University: K. Dehmelt, A. Deshpande, N. Feege, T. K. Hemmick
University of Virginia: K. Gnanvo, N. Liyanage
Yale University: R. Majka, N. Smirnov

Abstract

This report focuses on recent progress during the period July-December 2016.

Past

What was planned for this period?

Brookhaven National Lab

The primary goal for this period was to complete the analysis of the beam test data from the TPC/Cherenkov (TPCC) hybrid prototype detector we tested at the Fermilab beam test facility last April. Preliminary results were reported on during the last review period and the final results are now essentially complete. These results were presented at the 2016 IEEE Nuclear Science Symposium in November 2016 and will be published in the IEEE Transaction on Nuclear Science (TNS) in early 2017.
We also planned to pursue our work to optimize the zig-zag pattern for the GEM readout of the TPC. We planned to design several candidate zig-zag patterns and to have several fully operational PCB boards fabricated to test their performance. However, this involved transferring our original design that was produced at Stony Brook to the Instrumentation Division at BNL for modification, which consumed both time and resources. We also discovered that our new design was pushing the limits on what could be actually be fabricated by industry. Due to limited funding, both of these factors severely limited what we were able to accomplish.
We also planned to build a new X-ray scanning table for testing large GEM detectors in our lab. The scanner will provide a much higher rate for X-ray measurements and will greatly speed up the time it takes to measure various board readout patterns. This new scanner will also be made available to other members of our eRD3/eRD6 Collaboration.
Finally, we planned to test several candidate gasses that contain neon which reduces ion feedback in the TPC.

Florida Institute of Technology:

Forward Tracker (FT) GEM detector development:
The main goal in this work period was to finish the tests of small zigzag boards to find the zigzag geometry with the most linear position response and best spatial resolution and to present and publish results from this study, e.g. in the 2016 IEEE NSS. Then we were to apply that optimal geometry to the design of the large readout foil for the FT GEM prototype chamber and to have the foil produced at CERN.
Another project to finish was the static structural FE analysis for the mechanical aspect of chamber assembly, specifically with respect to any potential for buckling of the frames under stretching forces.
We were to choose proper materials for frames, support boards, and then to identify companies in the industry that can produce them for us. We also had planned to measure leakage currents of large common GEM foils received from CERN to assure the foil quality.
Finally, we were to phase out the participation of our post-doc Aiwu Zhang due to termination of his EIC R&D funding as directed by the review committee and project management.

INFN Trieste:

N/A

Stony Brook University:

The existing evaporator (Figure 1) that is routinely used for evaporating CsI on GEMs for HBD like readout structures, will be upgraded with electron-gun and ion-beam equipment to precisely control the evaporation of material on surfaces of mirrors: the cover material of the mirror, MgF_2 can be reliably attached to the surface of the prepared mirror blank plus aluminium.
For preparing this evaporator we are in the process to purchase an electron gun. The latter process requires the protection of areas that are serving as an insulator between conducting elements within the evaporator.
Another project was to design a pad readout board with a snowflake pattern, locally at Stony Brook with engineers and aiming for placing an order to our previous PCB vendor.

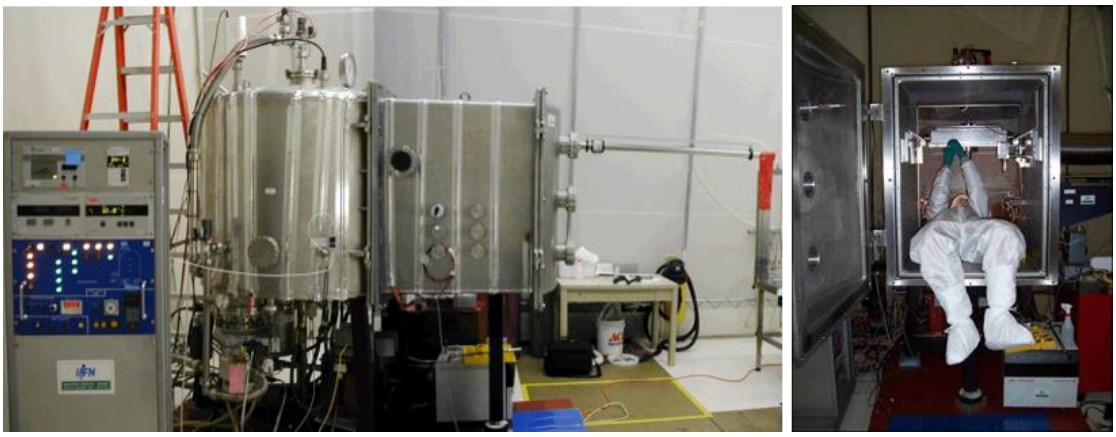

Figure 1 Evaporator in the clean room of SBU. Left: side view. Right; View inside the evaporator.

University of Virginia:

For the current cycle (June 2016 to December 2016), we planned to:

1. Continue the study of Cr-GEM detector with x-ray source. Take data under moderate particle rate for several months to study the long-term stability and aging of such thin Cr-GEM structures,
2. validate the new ideas such as etching the top and bottom strips contacts on the same Kapton support and the zebra connectors for electrical contacts developed for U-V strips readout of EIC GEM prototype II, on a small scale (10 cm × 10 cm) readout prototype before we move ahead with the full-size detector,
3. Upon reception of the UVa version of the EIC common GEM foils from CERN, perform HV tests of the foils for quality control. In the meantime, we would have completed the design of the frames and mechanical structure and the fabrication of the full-size U-V readout board is expected to be launched.

Yale University:

Finishing the write-up for the 3-coordinate GEM investigations.
Start investigating the 2-GEM plus Micromegas using resistive plane Micromegas readout.
Performing the multiple gating grid studies.

What was achieved?

Brookhaven National Lab

FNAL Beam Test Data Analysis

The main purpose of the beam test of the TPCC detector at FNAL was to provide a proof of principle for the operation of a hybrid GEM based TPC and a proximity focussed Cherenkov detector in a common gas volume. The TPC portion consisted of a quadruple GEM detector with a chevron readout plane with 2x10 mm^2 pads with zig-zag shaped electrodes. The Cherenkov portion consisted of a second quadruple GEM with a CsI photocathode that was mounted on a movable stage that allowed the distance from the Cherenkov GEM and the TPC to be varied. The readout plane for the Cherenkov detector consisted of a 3x3 array of pads, each measuring 3.3x3.3 cm^2. Figure 2 shows the inside of the detector and the chevron readout plane for the TPC. Incoming beam tracks were measured in a high precision silicon telescope that was provided by the test beam facility and used to measure tracks in the TPC detector in order to determine its position and angular resolution. The X coordinate was measured using charge sharing between the zig-zags in the 2 mm pad direction, and the Y coordinate was determined by measuring the drift time along the drift direction. The Z coordinate was determined simply by the pad spacing along the 10 mm direction. The detector vessel was filled with ultra-pure CF_4 gas that served as the radiator for the Cherenkov detector, as well as the drift gas for the TPC, and also as the operating gas for all the GEM detectors.

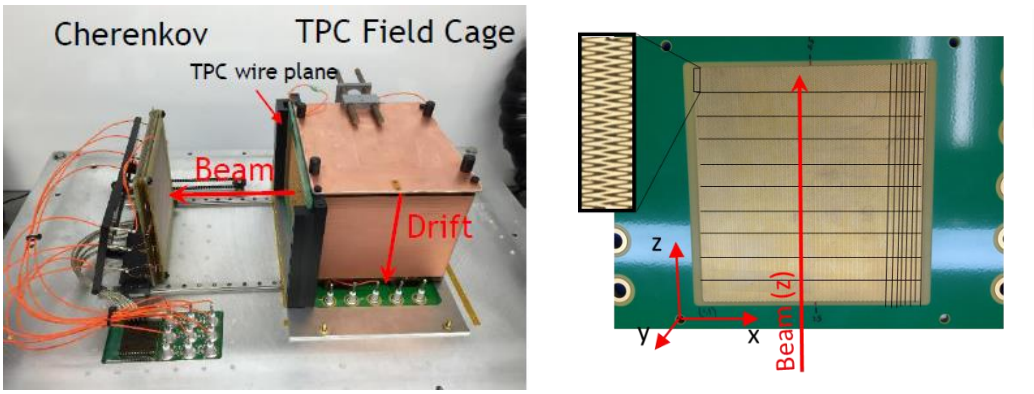

Figure 2 Interior of the TPCC prototype detector (left) and TPC readout plane (right).

Following the preliminary analysis of the TPC data presented in our last report, it was found that the detector was dominated by single pad hits due to the low transverse diffusion of CF_4, which severely limited the resolution. Secondly, it was found that the time window of the DAQ was set during data taking such that a portion of the beam profile was cut off. This limited our statistics but did not affect our ability to measure the resolution. Thirdly, it was found that the data files generated from the TPCC and the silicon detector DAQ systems were not fully synchronized event-by-event. Our subsequent analysis concentrated on improving the initial results by eliminating single pad hits, eliminating truncated tracks, and synchronizing the events from both DAQ systems. As part of this analysis, we were also able to successfully correct for the trigger-DAQ clock phase offset that had not been done in our earlier analysis, as well

as fixing several minor bugs and improving the offline alignment between the silicon detector and TPC.

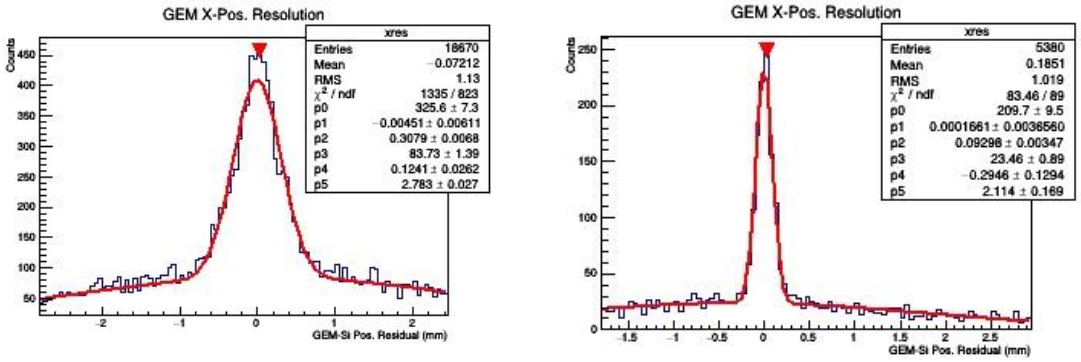

Figure 3 Position resolution before (left) and after (right) removal of single pad hits.

Figure 3 shows the position resolution in the X direction (i.e., along the 2 mm dimension of the zig-zag) before and after single pad hits are removed from the analysis, but before removal of unsynchronized events, which gives rise to the broad uncorrelated background under the peak. Removing the single pad hits results in a significant improvement in the resolution, from about 300 μm to about 90 μm, as shown in the right-hand plot. However, the improved resolution comes at the cost of efficiency, which drops from nearly 100% to 28%. As we discuss below, this could be substantially improved by using a gas with larger transverse diffusion and/or increasing the interleaving of the zig-zags.

Figure 4 shows the results of the position resolution once the TPCC and silicon detector DAQ events were synchronized. One can see that the background events are substantially cleaned up (compared with Fig. 7 in our July 2016 report). The resolution for the X coordinate improves to slightly less than 90 μm and the resolution for the Y coordinate is about 160 μm.

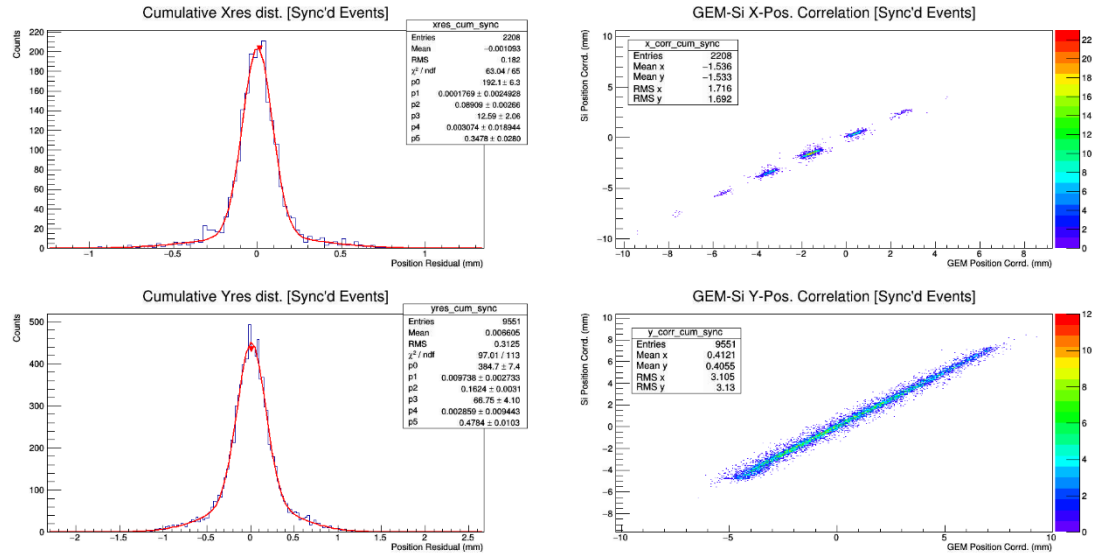

Figure 4 Left: Position resolution along X coordinate (top), and Y coordinate (bottom). Right: Correlation of track position in the TPC vs the silicon telescope for both the X (top) and Y (bottom) coordinates.

The Cherenkov mesh operates at about 4kV and is parallel to the wire plane of the TPC field cage, which operates between 4-8kV, and therefore has the possibility of affecting the drift field of the TPC if the two are in close proximity. We attempted to study the effect of the Cherenkov detector mesh on the quality of the track reconstruction, but unfortunately, the silicon detector was off during this measurement. However, we were able to study the spread in the reconstructed track angle as a measure of the quality of the reconstructed track. The spread in the reconstructed angle is essentially the same as the angular resolution since all tracks during a given run have essentially the same fixed incoming angle. Figure 5 shows the spread in the reconstructed angle as a function of the distance between the Cherenkov mesh and the wire plane of the TPC field cage. The resolution is essentially flat, indicating that the effect of the Cherenkov mesh potential on distorting the TPC drift field is negligible down to a distance of 18 mm.

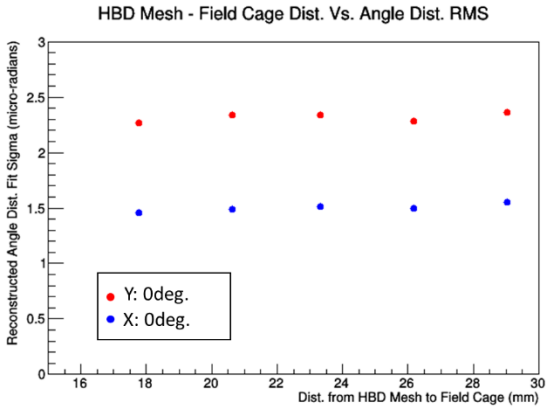

Figure 5 Reconstructed track angle in the TPC (as a measure of the reconstructed track resolution) versus the distance between the Cherenkov mesh and the TPC field cage.

Further analysis of the data from the Cherenkov portion of the detector was also carried out, which was done in collaboration with our colleagues from Stony Brook. In our previous report, we showed the correlation between tracks found in the TPC and hits found in the Cherenkov. We also showed preliminary data for the pulse height distributions from the Cherenkov section for particles above and below threshold at different operating voltages for the Cherenkov GEMs. However, we discovered during our analysis that these pulse height distributions were subject to significant common mode noise and also suffered from saturation in the readout electronics. We developed techniques to overcome these problems, which included common mode noise rejection and a method using the rising edge of the preamp pulse to estimate its true unsaturated amplitude. These methods seem to have worked rather well, and the pulse height distributions for the extrapolated corrected pulse heights are shown in Figure 6 for two different Cherenkov radiator lengths.

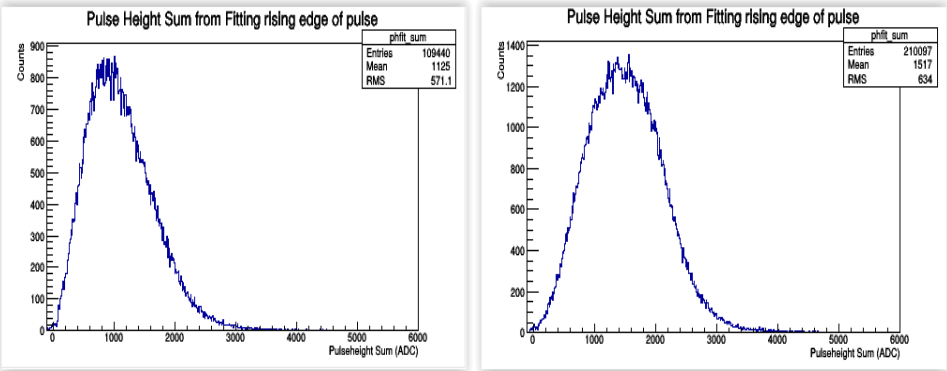

Figure 6 Pulse height distributions using the corrected pulse heights for an 18 cm (left) and 29 cm (right) radiator length.

The response of the Cherenkov detector was measured as a function of the radiator length in order to determine the photoelectron yield for the photosensitive GEM. The distance was varied from 18 to 29 cm, which not only provided the yield as a function of distance (which should vary linearly), but the intercept also provided a measure of the direct ionization detected by the track passing through the photosensitive GEM detector. This ionization has two components. One is from the small region above the photocathode from which charge is still collected even in reverse bias operation, and the other is the ionization produced in the first transfer gap (which receives a gain of only G^3 instead of G^4 from the full detector).

Figure 7 shows the summed pulse height distributions from all fired pads from the Cherenkov detector as a function of the radiator length. The relationship is indeed consistent with being linear. The intercept allows us to estimate the amount of direct ionization detected by the GEM using the published values for dE/dx in pure CF_4 and gives a value of around 4 electrons. Using this to convert ADC counts into photoelectrons, we find that the number of photoelectrons generated from Cherenkov light produced in 29 cm of CF_4 radiator is ~ 11.5. This is in excellent agreement with the expected number of 11.6 p.e. that is computed by scaling the number of photoelectrons measured in the PHENIX HBD by the respective radiator length, p.e. collection efficiency, mesh optical transparency, and GEM surface area of both detectors.

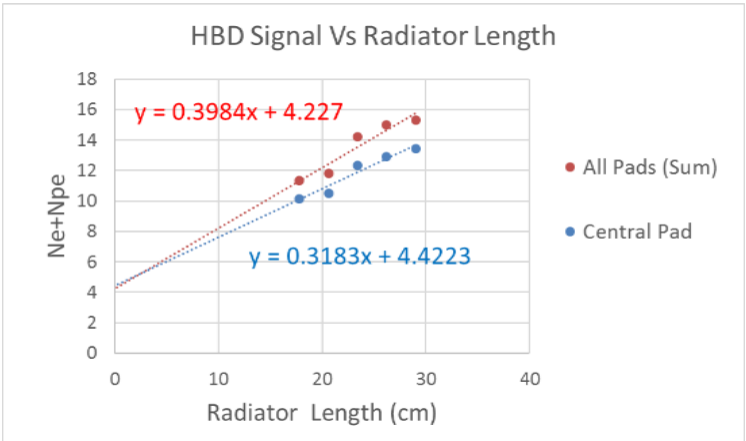

Figure 7 Total number of electrons produced by direct ionization and photoelectrons produced by Cherenkov light versus radiator length. The number of direct ionization electrons from the intercept was used to convert ADC counts to electrons for computing the photoelectron yield.

Zig-zag GEM readout

We also continued our investigation of chevron "zig-zag" readout patterns. The chevron pattern used for our prototype TPC was based on the pattern that was used for the LEGS TPC, and was also used in our study of the minidrift GEM detector which has been described in previous reports and is now published (IEEE Trans. Nucl. Sci. Vol. 63, No.3, June 2016, pp. 1768-1776). With the minidrift, we were able to achieve a spatial resolution of less than 100 μm for small angle tracks and ~ 350 μm for tracks up to 45°. However, this was using an Ar/CO_2 gas mixture which provides reasonable transverse diffusion over a short drift distance. In the case of the TPCC, we used pure CF_4, which provides very little transverse diffusion even over the full 10 cm drift. This is evident by the poor resolution observed when including single pad hits and the significant improvement in the resolution when eliminating single pad hits as shown in Fig. 2. In addition, as is discussed in our minidrift paper, there was a significant differential non-linearity observed with the chevron pattern used with the minidrift detector which had to be corrected for.

We have investigated ways of improving the resolution of the chevron readout patterns by studying some of the fundamental limitations of their performance. This involved Monte Carlo simulations of various zig-zag geometries. The purpose was to optimize the zig-zag pattern of the chevron readout plane for a future full-size TPC where there will be other constraints on the design, such as limiting the total number of readout channels, optimizing the resolution for tracks over a fairly wide range of angles, and reducing ion feedback. In this initial study, we focused the performance criteria mainly on the degree of linear response and the level of charge sharing between the electrodes. Figure 8 illustrates an idealized case of a very high degree of overlap between the zig-zags and no gaps between the electrodes. The pink circle on the left represents a charge cloud with a sigma of 400 μm, and the plots on the right show that a spatial resolution ~ 60 μm can be achieved with virtually no differential non-linearity.

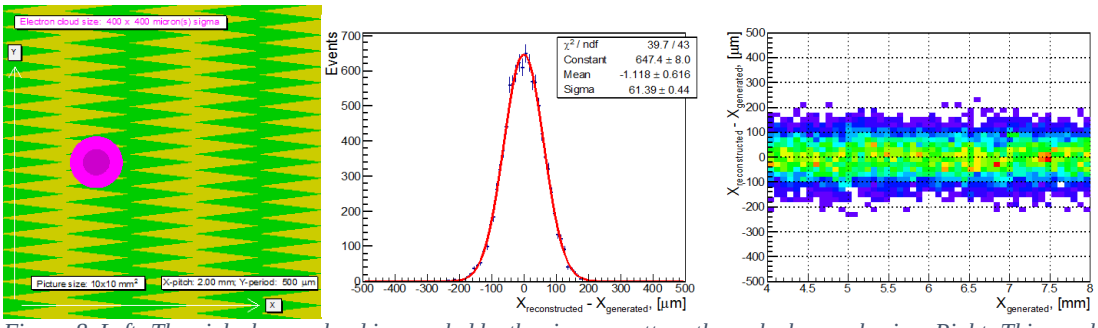

Figure 8 Left: The pink charge cloud is sampled by the zig-zag pattern through charge sharing. Right: This results in a narrow residual distribution ($\sigma \sim 60$ μm) and a flat response across the zig-zags.

However, in a practical design, there must be gaps between the zig-zag electrodes which will affect the performance of the readout. Figure 9 illustrates a set of parameters that can be used to specify the zig-zag pattern. In order to optimize the resolution and differential non-linearity, one would like to have a minimal gap spacing and a maximum amount of overlap. The gaps also cause a distortion of the electric field near the electrodes, so one does not want to reduce the amount of copper area too much.

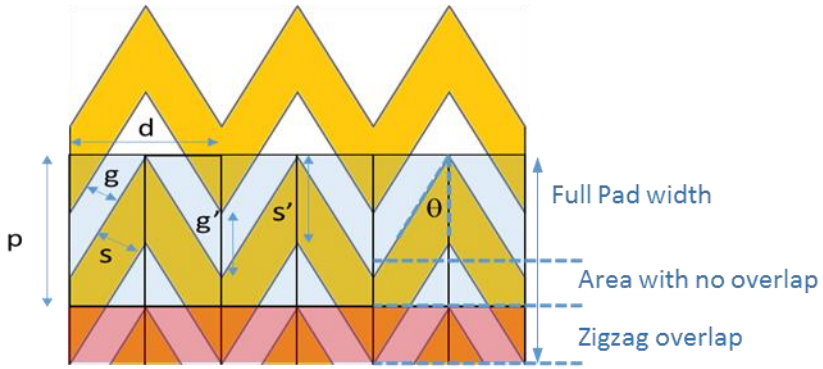

Figure 9 Parameters used to characterize the zig-zag pattern: p=pad pitch, d=zig-zag pitch, s=trace width, and g=gap width. The red region shows the region of overlap between neighboring pads.

We met with several high-quality PCB manufacturers and discussed with them what their limitations were in fabricating this type of readout board. We learned that it was essentially impossible to go below a gap spacing of .002", which can in principle be achieved using advanced but expensive laser etching, but .003" was the standard limit for chemical etching. We, therefore, developed a readout pattern which had 0.003" gaps with 94% zig-zag overlap and 70% copper area coverage, as shown in Figure 10, and have submitted this design for fabrication of a 10x10 cm^2 readout board with 2x10 mm^2 pads. This board will incorporate our standard 10x10 cm^2 GEM configuration and can be used with both our TPC and minidrift prototype detectors. In addition, we developed several other readout designs that we would like to test on a simple 2 layer PCB to explore the limits of what can in principle be produced by industry for an actual readout board. An example of some of these patterns is shown on right in Figure 10. However, due to limitations in our budget, we were not able to have any of the 2 layer boards fabricated at this time.

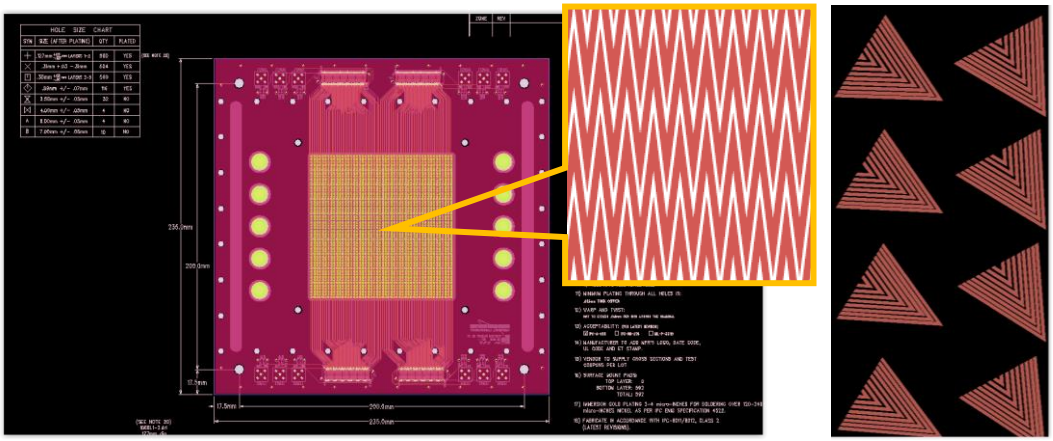

Figure 10 Left: Layout design for the PCB that was sent out for fabrication, including a blow-up of the employed zig-zag pattern with .003" gaps, 94% zig-zag overlap and 70% copper area coverage. Right: Portion of a test pattern to be used for testing fabrication limits on a 2 layer PCB.

New X-ray scanner

We purchased a new X-ray generator and constructed a new scanning table that will allow us to scan larger area GEMs (up to 38x38 cm^2) and with much higher rates than was previously possible with our existing scanner. The new X-ray generator has a 40W X-ray tube compared with a 3W X-ray tube in our current generator. This will allow us to perform scans in a matter of a few hours which previously took up to several days. The new setup, shown in Figure 11, is currently being assembled and should be

operational in early 2017. We also plan to make this facility available to other eRD3/eRD6 collaborators.

Figure 11 New X-ray scanning table capable of scanning up to 38x38 cm2 GEMs with high DAQ rates using a new 40W X-ray generator.

Gas studies

A full-size TPC at EIC will have to deal with high ionization levels in the gas due to the very high luminosity of the EIC collider. It will, therefore, be important to limit the ion backflow into the drift volume under such conditions, and we are exploring various

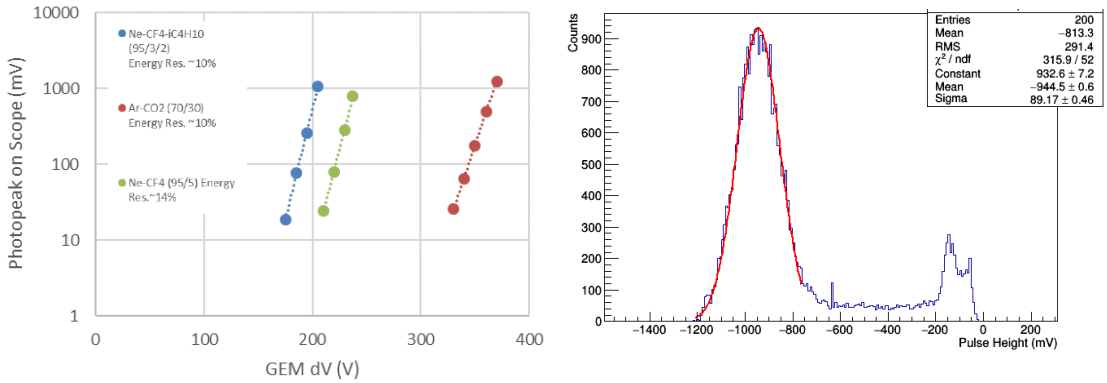

Figure 12 Left: Gain curves for two possible Ne based gas mixtures compared with a standard Ar mixture. Right: Pulse height distribution for a 4 stage GEM using the Ne2K gas and giving a resolution of 9.4% for 55Fe. The small peak at ~150 mV is due to conversions in the first transfer gap.

ways to accomplish this. These issues have also been addressed by the ALICE collaboration at LHC and are being studied by the sPHENIX Collaboration for their TPC.

Since the ion mobility varies inversely with the mass of the ion (actually $1/\sqrt{\mu}$, where μ is the reduced mass of the gas molecule), the ion backflow can be reduced by utilizing a gas with lighter molecular weight, such as neon instead of argon. This has been the approach taken by the ALICE experiment, which is planning to use a mixture of $Ne/CO_2/He$, and most likely by sPHENIX, which has been investigating a "Ne2K" mixture ($Ne/CF_4/i\text{-}C_4H_{10}$), which is similar to the gas used by the T2K experiment, but

replacing Ar with Ne. We have studied two possible Ne mixtures in a 4 stage GEM detector and found that we can achieve high gain and good energy resolution with very stable operation. Figure 12 shows results from some of these preliminary measurements. The plot on the right is the pulse-height distribution obtained with a ^{55}Fe source and gave a resolution of 9.4%.

Florida Institute of Technology

1. Response optimization of FT zigzag readout strips with small PCBs

We measured the spatial response linearity and spatial resolution of six small readout boards with different zigzag strip geometries using a 10×10 cm^2 triple-GEM detector with 3/1/2/1 mm gap configuration. The detector was mounted on a 2D motorized stage and exposed to a highly collimated X-ray beam (140 μm × 8 mm slit) at BNL. Two of the boards had the same design as the readout in our first 1-meter zigzag-GEM prototype that was tested in a beam at FNAL in 2013; they showed strong non-linear responses as discussed in our last report (June 2016). Potentials on electrodes were supplied with seven individual HV channels. The voltages were set as if an HV divider (with resistances 1/0.5/0.5/0.45/1/0.45/0.5 MΩ) was used so that setting one voltage on the drift (V_{drift}) determined all fields in the GEM detector. This way we kept the configuration as it was in the 2013 beam test for better comparison.
We improved on the original zigzag strip design by extending the zigzag tips to the centers of both adjacent strips, which we refer to as a design with "100% interleaving". As discussed in previous reports and presentations to the review committee, proper interleaving is crucial for good charge sharing among strips and consequently for spatial linearity and resolution.
For versatility, the PCB was designed with two different radial strip geometries. On the left side of the board, the radial strips were arranged with an angle pitch of 4.14 mrad corresponding to the planned strip layout near the inner radius (206-306 mm) of the next FT GEM prototype, while on the right side of the board radial strips were arranged with an angle pitch of 1.37 mrad corresponding to the layout of the outer radius (761-861 mm) of the future full-size prototype.
During the course of working with industry to have such a PCB produced, we found that the design was pushing the limits of industrial PCB production capabilities since the strong interleaving requires the spaces between adjacent strips to be less than 3 mils (76 μm). In the end, for the three versions of the boards produced by PCB company Accurate Circuit Engineering (ACE), the actually achieved interleaves were 90%, 94%, and 117% (Figure 13).
We also had a board with the same design produced at CERN, in which the zigzag strips were implemented on a Kapton foil instead of on a PCB. The foil was then glued onto a honeycomb board for support at CERN. The main reason for producing this board is that currently CERN is the only place that can produce 1-meter-long designs on a Kapton foil as required for our next FT GEM prototype. Consequently, this small board served essentially also as a pilot project to see if CERN can produce the zigzag strip structures with sufficient accuracy.
Figure 13 shows microscopy photos of the boards from ACE and CERN. The first board (ACE #1) was produced using a standard PCB etching method, where the copper thickness was about 18 μm (1/2 oz.). In this board the tips were overetched, so they were not fully reaching the adjacent strip centers. The estimated interleaving between zigzag strips was 90%. ACE board #2 was produced by using half the copper thickness

(9 µm, 1/4 oz.) compared with ACE board #1. The resulting interleaving of ~94% is the closest the company could achieve. For board ACE #3, we tried to directly compensate in the design for the over-etching problem; however, the strips became too thin and the interleaving came out significantly larger than 100%. Finally, the CERN foil board achieved an interleaving of ~95%, which was an encouraging outcome.

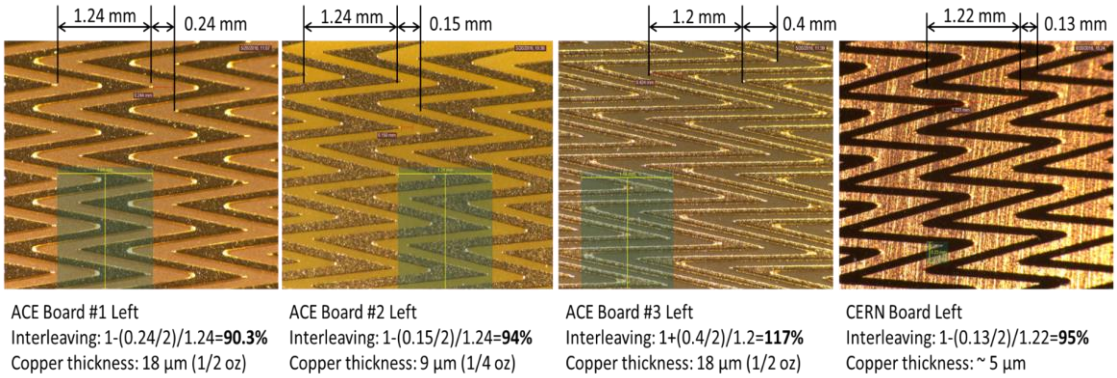

Figure 13 Microscopy photos of the zigzag readout structures produced at a PCB company (ACE) and at CERN. Vertical lines indicate strip pitch and distance between tips that are used to determine the amount of strip interleaving.

Figure 14 and Figure 15 show the measured mean strip cluster centroids for ACE board #2 and the CERN board vs. the X position of the X-ray beam across the zigzag strips. We typically scanned across 2-3 strips with a 100 µm step size. At each position, only data for events with single hits were acquired. The plots on the left are for strips with angle pitch 4.14 mrad that start around radius r = 229 mm, while the plots on the right side are for strips with angle pitch 1.37 mrad that start near radius r = 784 mm. Results are compared for cluster strip multiplicities 2, 3, and overall, but excluding single-strip clusters (>1). The small flat regions in the plots are due to motor backlash encountered during the scans when data taking was interrupted. The spatial response is found to be much more linear with the optimized zigzag design than with the original zigzag design (see the previous report, June 2016).

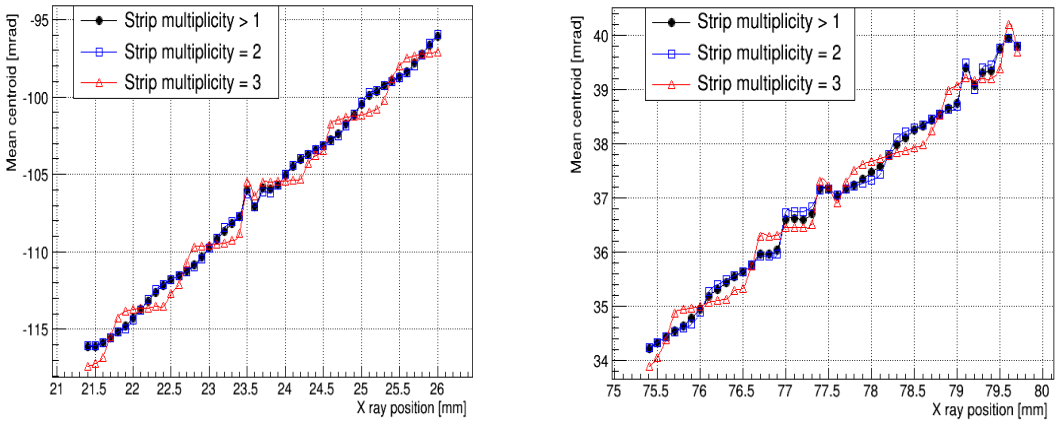

Figure 14 Mean strip-cluster centroid as a function of X-ray position for ACE board #2 in the scan across zigzag strips. Results for 2-strip, 3-strip and strip multiplicity >1 clusters are shown. On the left, strips have angle pitch 4.14 mrad and starting radius 229 mm. On the right, strips have angle pitch 1.37 mrad and starting radius 784 mm.

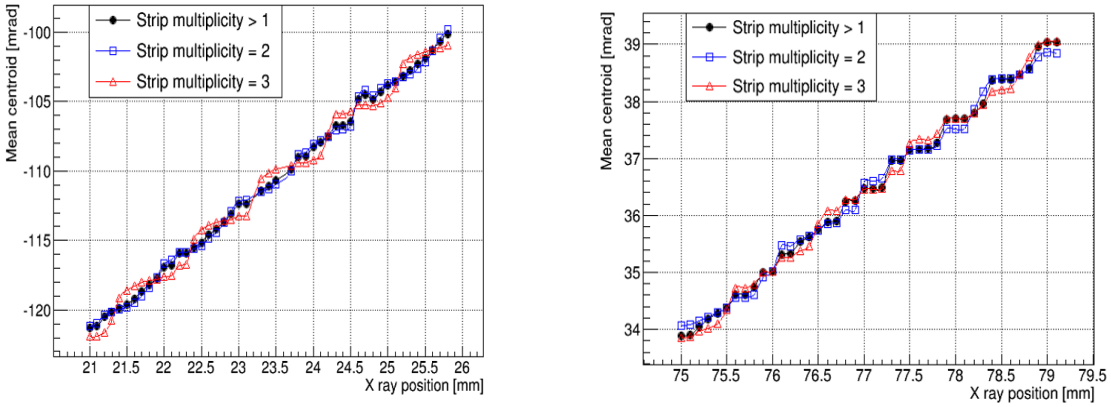

Figure 15 Mean strip-cluster centroid as a function of X-ray position for CERN board in the scan across zigzag strips. Results for 2-strip, 3-strip and strip multiplicity >1 clusters are shown. On the left, strips have angle pitch 4.14 mrad and starting radius 229 mm. On the right, strips have angle pitch 1.37 mrad and starting radius 784 mm.

Figure 16 shows the measured mean cluster strip multiplicities in the scans across strips for ACE board #2 and CERN board. We observe a comb-like pattern as the X-ray position moves across the zigzag structure as expected. The vast majority of the clusters have more than one strip fired, typically two to three strips, which allows for charge sharing and improves the accuracy of the centroid measurement. Figure 17 and Figure 18 show resolution studies for the CERN board for strips with angle pitch 1.37 mrad for 2-strip and 3-strip clusters, respectively. The raw residuals are calculated from these and the residual widths are found to be 80 µrad (2-strip) and 112 µrad (3-strip).

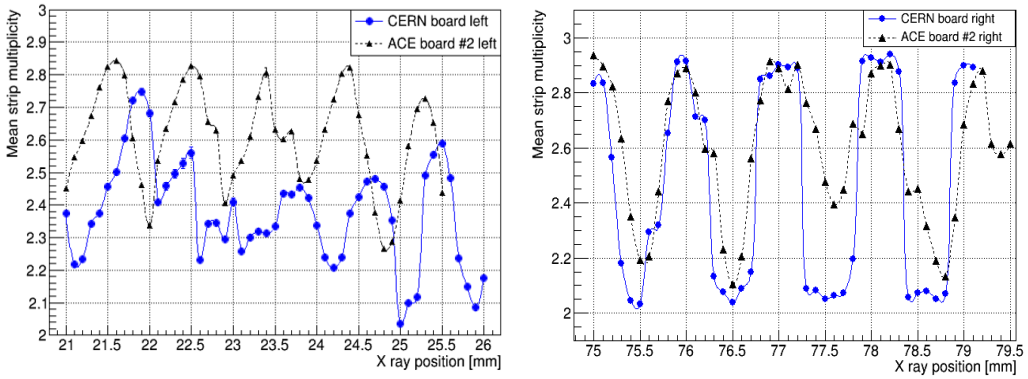

Figure 16 Mean strip multiplicity vs. X-ray position for ACE board #2 and CERN board in the scans across strips. Left (right) is for strips with angle pitch 4.14 mrad (1.37 mrad) and starting radius 229 mm (784 mm).

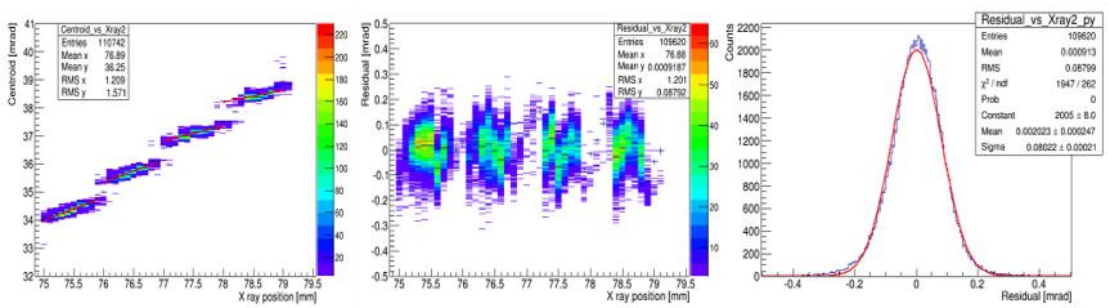

Figure 17 Resolution study for 2-strip clusters with the CERN board for the strips with angle pitch 1.37 mrad. Left: centroid vs. X-ray position. Center: residuals vs. X-ray position. Right: residual distribution of all selected events.

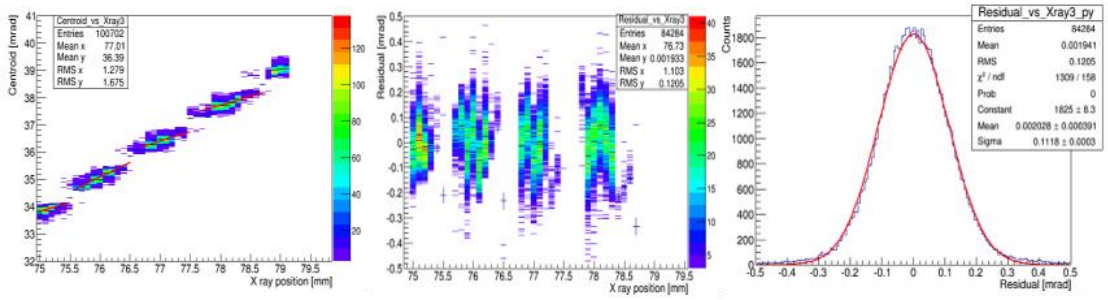

Figure 18 Resolution study for 3-strip clusters with the CERN board for the strips with angle pitch 1.37 mrad. Left: centroid vs. X-ray position. Center: residuals vs. X-ray position. Right: residual distribution of all selected events.

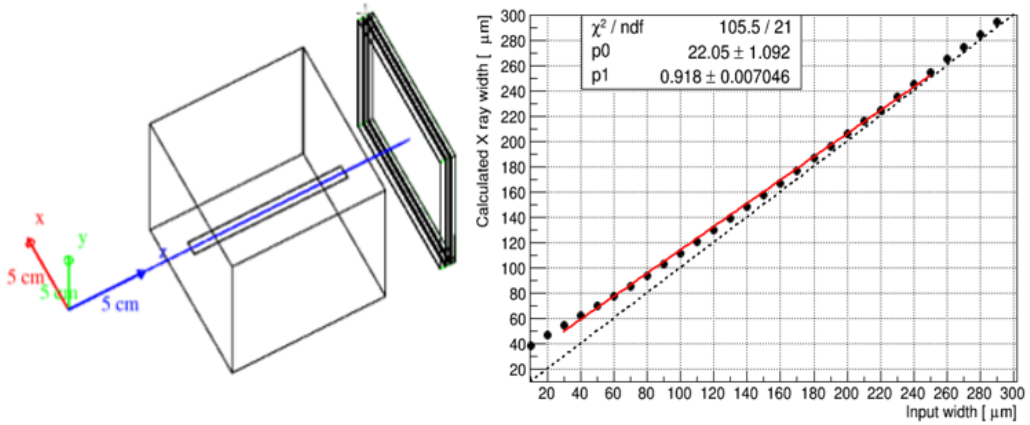

Figure 19 Geant4 simulation of the effect of X-ray collimator on detector resolutions.

In order to get the actual spatial resolutions for the tested zigzag boards, we need to subtract the effect of the finite width of the X-ray collimator, which causes a smearing of the X-ray incidence position on the detector. This is done with the help of a simple Geant4 simulation. Figure 19 shows the geometry in Geant4 and the simulation result. Through the simulation, the relation between intrinsic detector resolutions that is fed into the simulation and measured width of the X-ray spot on the detector is determined. This mostly linear function is then used to obtain the actual spatial resolution from the measured raw residual width. The finite width has an impact mainly below 100 µm. A few different X-ray beam shapes emerging from the source (uniform rectangular, cone, Gaussian-distributed) are tested and their impact is found to be negligible.

The final spatial resolutions for all boards scanned across the strips are summarized in Table 1. Clusters with two strips and three strips are calculated separately as well as combined. We find that the overall spatial resolutions are well below 100 µm.

Table 1 Spatial resolutions for all boards from scans across zigzag strips. Effects due to finite X-ray collimator width are subtracted. Statistical errors are less than 0.3%. The applied drift voltage and approximate gas gain are listed. The gain between setups varies by about 1000 for different boards due to changes of gas and flow rate.

Spatial resolution (µrad/µm)	V_{drift} (V)	Approx. gas gain	Strips with angle pitch 4.14 mrad, r ≈ 229 mm			Strips with angle pitch 1.37 mrad, r ≈ 784 mm		
			2-strip clusters	3-strip clusters	2 & 3-strip cl.	2-strip clusters	3-strip clusters	2 & 3-strip cl.
ACE #1	3380	4000	266 / 61	371 / 85	328 / 75	56 / 44	69 / 54	60 / 47
ACE #2	**3340**	**3000**	**288 / 66**	**480 / 110**	**384 / 88**	**57 / 45**	**97 / 76**	**84 / 66**
ACE #3	3250	1500	-	572 / 131	-	-	140 / 110	-
CERN	**3340**	**3000**	**397 / 91**	**393 / 90**	**397 / 91**	**-**	**-**	**-**
CERN	**3380**	**4000**	**-**	**-**	**-**	**57 / 45**	**92 / 72**	**71 / 56**

We also performed scans along the zigzag strip direction for the various boards to investigate biases associated with the incidence position along a strip. Here we scanned a length of 3.5 mm that corresponds to seven multiples of the 0.5 mm periodicity of the zigzag structure of a single strip. Figure 20 and Figure 21 show the results for the CERN board as an example. The overall curve has a slope that is due to the fact that the scanning was done along a direction (Y) perpendicular to the direction (X) across the strips, which was not exactly a radial direction. This scan direction was dictated by the Cartesian setup of the scanning stage.

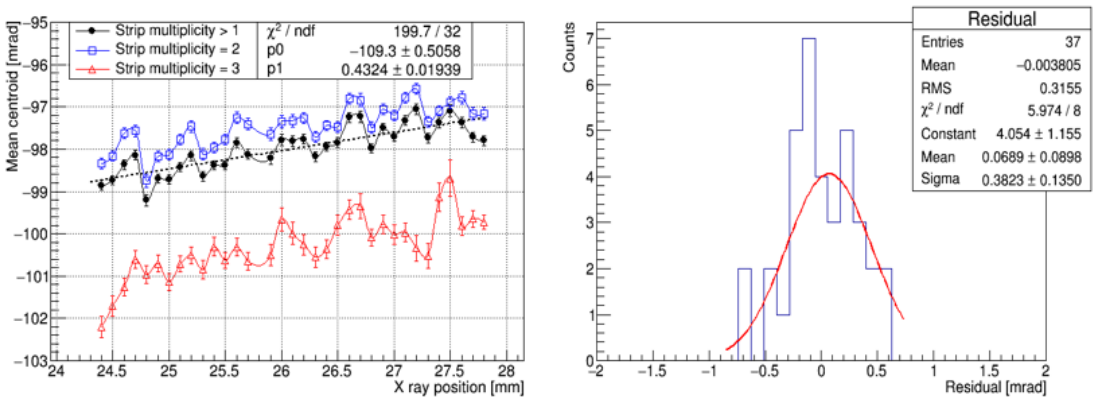

Figure 20 Left: mean centroid as a function of X-ray position in the scan along a zigzag strip with angle pitch 4.14 mrad on the CERN board. Right: histogram of residuals of mean centroids for >1-strip clusters from all scans.

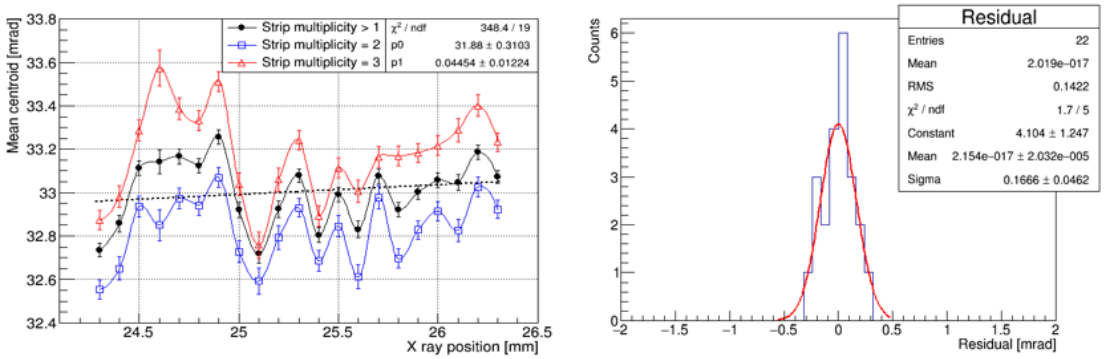

Figure 21 Left: mean centroid as a function of X-ray position in the scan along a zigzag strip with angle pitch 1.37 mrad on the CERN board. Right: histogram of residuals of mean centroids for >1-strip clusters from all scans.

The mean centroid is found to oscillate as a function of X-ray position along the strip with a period similar to the 0.5 mm periodicity of the zigzag structure along the strip. A line was fitted to the mean centroid for >1-strip clusters so that the residuals could be calculated. The overall RMS width of the residual distribution is a measure of this oscillation, i.e. of the systematic mismeasurement of the X position across strips due to the Y position along the strip.

For the >1-strip clusters case, this bias is about 382 μrad (87 μm) for strips with angle pitch 4.14 mrad, which is comparable to the spatial resolution itself as discussed above. In the case of angle pitch 1.37 mrad (at r ≈ 784 mm), the observed mismeasurement is 167 μrad (131 μm), which is more than twice the spatial resolution itself and consequently dominates the precision of the X measurement at large radii.

These results were presented in a poster at the 2016 IEEE NSS in Strasbourg, France. Due to lack of funding and restrictive DOE rules for attending international conferences, we could not travel to the conference, but the poster was presented on our behalf by RD6 consortium colleague Martin Purschke (BNL).

A publication draft on the results shown here has been prepared and is currently under internal review.

2. Status of construction of the next full-size EIC FT GEM detector prototype.

We finished mechanical design and stress analyses of the new chamber design using Autodesk Inventor. Undergraduate student Matt Bomberger has been trained on this project. Results show that our design based on carbon fiber frames should not suffer from substantial deformations due to foil tensions.

We received four common FT GEM foils from CERN in July 2016. Their leakage currents were tested with a Megger Gigaohmmeter at 500 V in the open air and all were found to be acceptable.

The circuit design of the 1-meter-long zigzag readout foil had to be revised substantially since CERN determined that they could not reliably produce very small vias over such large area. The revised version was sent to CERN and accepted by Rui De Oliveira's team in December 2016 and is now ready for production in early 2017.

We prepared for the production of the carbon fiber frames for the detector. Two laminated plywood boards with precision holes were produced that will serve as templates for carbon fiber frame production. We have teamed up with a faculty member in mechanical and aeronautical engineering at Florida Tech, who is an expert in composite materials such as carbon fiber.

We identified local company Tru Mension Manufacturing Solutions (TMM Inc.) for producing the remaining mechanical components for chamber assembly. These include halogen-free FR4 frames, pullout posts, screws, and so on.

INFN Trieste:

N/A

Stony Brook University:

All needed equipment has been identified as well as the specifications for installing the equipment in the evaporator have been established. At the write-up of this report, the purchase of the ion-beam equipment has been done and the purchase of the electron-gun equipment is under way. We obtained 50 mirror blanks of lightweight carbon fiber reinforced polymer. These will be placed in strategic positions on a frame that resembles a typical large mirror blank. We also obtained a commercially produced mirror with certified reflectance which will serve as an absolute calibration device.
In collaboration with BNL, we produced the Cherenkov-GEMs and participated in the test beam campaign in April 2016 for the BNL TPCC effort which was described in the BNL portion of this report. We have presented the results of this test beam effort at the IEEE NIS/MIC conference in Strasbourg in November 2016. We are participating in the production of a journal paper of the TPCC efforts and produce the proceedings write-up of the IEEE presentation.

University of Virginia:

1.**R&D on Chromium GEM (Cr-GEM)**

Cr-GEMs are foils where the Copper layer on both sides of the active area a standard GEM foil have been removed, leaving only about 100 nm thick residual Chromium

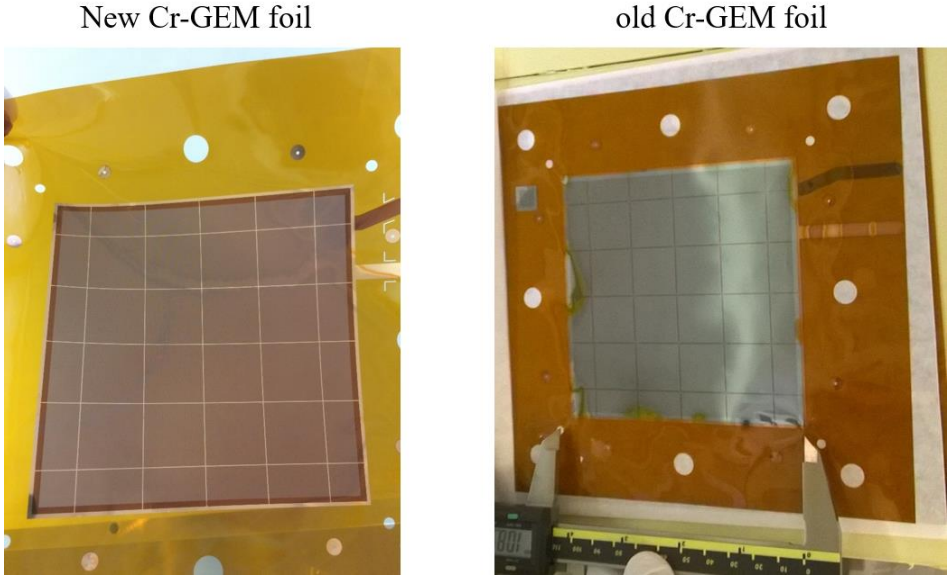

Figure 22 A Cr-GEM foil from the new batch (left picture) compared to a foil from the old batch (right picture).

layer used as electrode. A Copper grid is nevertheless needed to ensure good electrical contact throughout the active area.

We have received a new batch of 3 Cr-GEMs from CERN to assemble a small triple-GEM chamber (proto II). As one can see in Figure 22 the new foils differ significantly in appearance from the ones that we got from CERN a year or so ago to build and test the first prototype. The active area of the old Cr-GEM foils has a silver color (Figure 22-right) which is the characteristic color of the Cr layer while for the new batch (Figure 22-left), the color of the active area is brown, suggesting that the Chromium layer might have been also significantly wiped out during the etching of the Copper. Electrical tests were performed on the new Cr-GEM foils and showed an uncharacteristically low charging current value when the HV is applied, indicating that a significant portion of the active area might not be actually covered with the Chromium conductive layer. We contacted the GEM workshop at CERN to discuss the issue with the foils. They were not able to explain the reason of the brownish color but they accepted to replace these foils with a new batch of good quality foils.

Assembly of the 10 cm x 10 cm triple GEM chamber with Cr-GEMs: We have decided to go ahead and to build a small triple-GEM chamber with the "bad" foils and to study the detector response. The preliminary results with cosmic and x-ray were unsuccessful as we were not able to detect any signal in the chamber. This confirmed our suspicion that the new foils were of very poor quality and the Cr layers have been probably etched out. Our next step, while waiting for the replacement of the Cr-GEMs has been to swap the 3 bad foils with the two undamaged Cr-GEM foils from the first batch and a standard GEM (with Cu electrodes) as third GEM foil to study the long-term stability of this hybrid setup. The primary R&D goal is to study the aging of Cr-GEM under moderate particle rate with the x-ray source. We have the chamber in the x-ray setup and intend to keep it for a couple months to monitor the gain uniformity and stability on a daily basis. The analysis of the accumulated data over a long period of time will help us understand the "evaporation" of the Cr layer observed with the prototype I after a few days of exposure to extremely high rate x-ray.

2.EIC U-V strip readout small prototype

We have received the small 10 cm × 10 cm U-V strip readout board and all the parts needed for the new zebra connection scheme. Figure 23 shows a picture of the readout board with the characteristics of the U-V strip pattern. The U-V strip readout is a small replica of the readout layer of the large EIC GEM prototype II designed around the new GEM foil developed commonly by UVa, FIT and Temple U's eRD6 / eRD3. The readout is based on the same technique used for the first EIC-GEM prototype but has a smaller pitch (down to 400 μm from 550 μm) as well as smaller strip's width for the U and V strips (from 140 μm and 490 μm to 80 μm 350 μm respectively). The U/V angle has also changed from 12º to 30º. We expect the combination of these changes to significantly improve the spatial resolution in both the radial and azimuthal direction. In addition, the new zebra connection scheme that we are testing will allow concentrating all front-end (FE) electronics needed to read out the detector's readout strips at the outer radius edge of the chamber. This will allow not having readout electronics in the active region of the detector. This is critical to reducing the risk of radiation damage to the FE electronics as well as reducing material contributing to multiple scattering and the dead zones in the sensitive area.

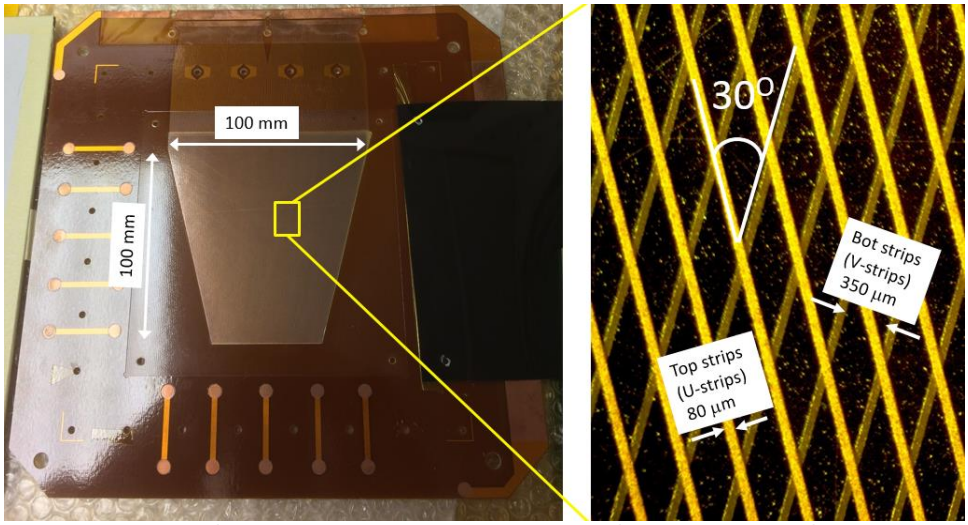

Figure 23 Small prototype of the new EIC U-V strip readout board (left) Characteristics of the U and V strips are shown (right).

Another feature of the zebra connection is that it does not require connectors soldered on the readout layer of the detector and access of the zebra contact on both side of the readout foil eliminates the need for conductive vias through the Kapton foil. A via-free and connector-free readout board is a critical advantage for large GEM chambers with a large concentration of readout strips as it significantly reduces the risks associated with channel loss through short vias contacts or bad soldering during fabrication and connector damage during operation of the chamber.

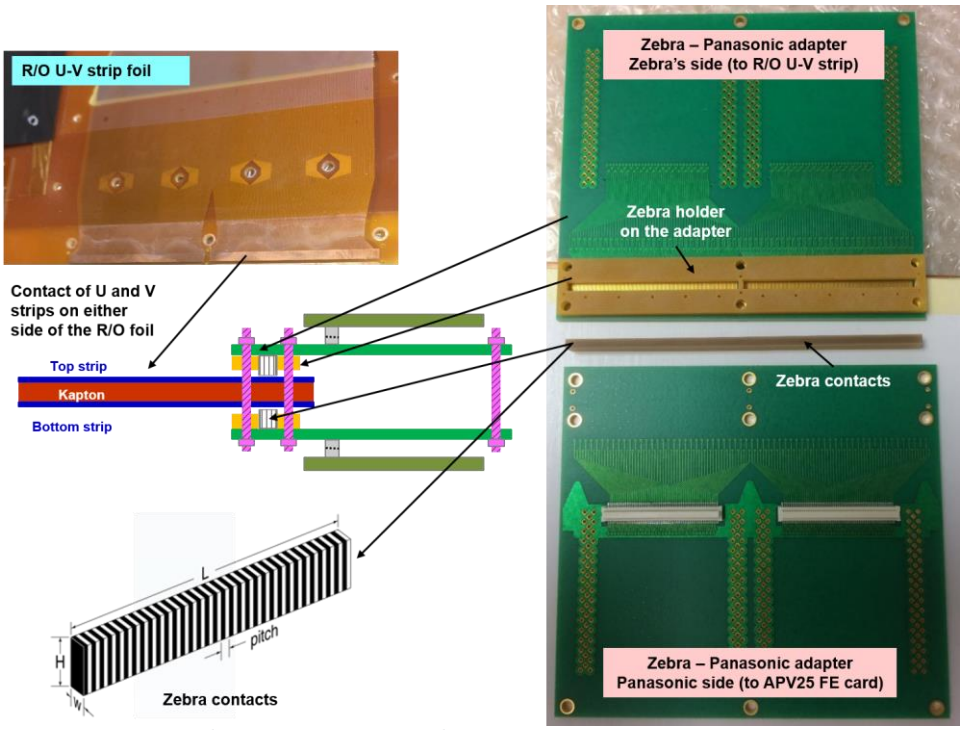

Figure 24 Components of the zebra connection of the EIC U-V strip readout board and assembly principle.

The different components of the zebra connection scheme are shown in Figure 24. The zebra strip which is the main part of the system is made of alternating layers of conductive and non-conductive silicone rubber with a pitch significantly smaller than the pitch of the electrical contact pad of the readout strips. This way, each pad of the readout strip layer will be in electrical contact with at least on the conductive layer of

the zebra strip. For our readout design, the contact pads of the U and V strips are on either side of the polyimide (Kapton) foil. The foil is sandwiched between two sets of zebra contacts previously inserted in holder frames and placed between two adapter boards facing each other on either side of the readout foil as illustrated in Figure 24. The inner side of the adapter has a matching pads pattern identical to the contact pads on the readout foil. The outer side of the adapter has the 130-pins Panasonic connectors for the APV25-SRS FE cards. A set of screws and nuts are used to adjust the pressure on the adapter boards to ensure good electrical contact between the zebra and the strip pads on both sides of the readout board on one hand and between the zebra and the matching pads on the adapter boards on the other hand. The adapter board also provides mechanical support of the whole structure.

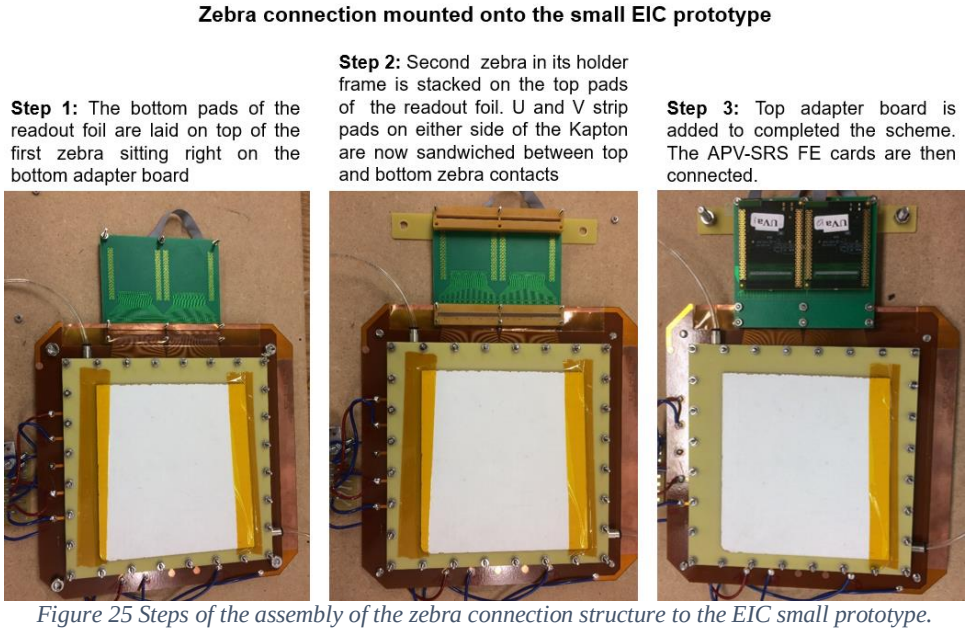

Figure 25 Steps of the assembly of the zebra connection structure to the EIC small prototype.

We have assembled a 10 cm × 10 cm triple-GEM prototype using spare GEM foils with the EIC U-V strip readout board and connected the zebra structure. Figure 25 shows the steps for the mounting of the zebra structure to the small EIC-GEM prototype

Preliminary tests of the small EIC prototype with cosmic

After the standard tests of the newly assembled prototype were validated, we placed the prototype on the cosmic setup and took some initial data to evaluate the signal quality of new zebra connection and to study effects such as the noise induced by this type of connection. Figure 26 shows a typical signal from cosmic in the small prototype with EIC U-V strip readout and the zebra connection scheme. First look at the cosmic data shows a significant improvement of the charge sharing between the top (U-strips) and bottom (V-strips) strips when compare to the first U-V strip readout design used in the first large EIC GEM chamber prototype. We also expect a larger cluster size (average number of strips with a hit from a cosmic event) to improve the spatial resolution of the detector. The analysis of the cosmic data is still ongoing for the full characterization of the prototype with the zebra connection concept before we implement it at a larger scale for the full-size EIC GEM prototype II.

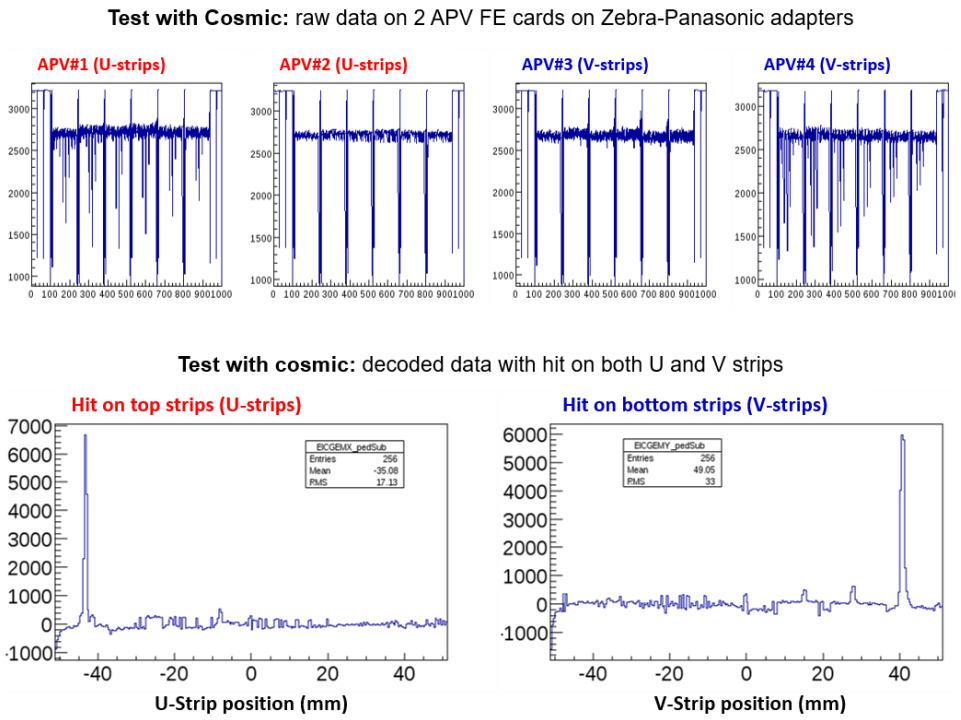

Figure 26 Top plots: raw APV data seen on two of the four APV25 FE cards connected to the chamber through zebra-Panasonic adapters; Bottom plots: decoded data with the cluster of hits in U and V strips from charge sharing between top and bottom strips.

Yale University:

1. 3d-Coordinate GEM

The analysis of test-beam data was done.
The result is prepared for the publication and will be submitted in 1-2 months.

2. Hybrid Gain Structure for TPC read-out – 2 GEMs plus Micromegas (2-GEMs + MMG)

A lot of results for different transmission E-fields, gas amplification, and gas mixtures were systematized and published (NIM).
Additional, presentations were done at RD-51 (CERN) meetings and ECFA collaboration workshop (invited report).
The first test was done for MMG with a resistive layer protection: TPC read-out style – R-strip was prepared for each TPC pad-row. The preliminary result demonstrated a very low HV PS „sensitivity“ to MMG sparking - ~0.3 V drop for ~ 300 ms.

What was not achieved, why not, and what will be done to correct?

Brookhaven National Lab

As stated above, we have now completed our analysis of the test beam data for the TPCC prototype detector and we are now in the process of writing up these results for publication in the IEEE Transactions on Nuclear Science.
The main area where we felt that we did not make as much progress as we had hoped was the study of the new chevron patterns. Our previous chevron pattern has been adopted from the LEGS TPC and implemented in our board design by an engineer at Stony Brook who has now retired. We, therefore, had to transfer this design to a new engineer in the Instrumentation Division at Brookhaven. This took a considerable amount of time, as it also involved having to locate and convert all the previous design files. It was also a very expensive process since we had to pay for the Brookhaven engineer's time out of our limited R&D budget. Fortunately, much of this time was invested in setting up the new design with the appropriate design tools and now making changes to the design will be rather simple and straightforward.
In addition, when we talked with the various PCB manufacturing companies, we learned that our design was pushing the limits of what they could fabricate and only a few better quality PCB board manufacturers could produce these boards. We had hoped to have several boards produced with different readout patterns, but the cost of the design and manufacture limited us to only being able to produce a single board. This board was submitted through the BNL purchasing system in mid-December and we expect delivery by early February. We also developed a number of other readout patterns that have the potential of further increasing the performance of the chevron readout. These designs push the limits of the capabilities of the board manufacturers, but they could be tested on a simple 2 layer board. However, the amount of funds available did not allow us to pursue any of these designs at this time, but we hope that additional funding will be provided during the next funding cycle to allow us to pursue more of these options.

Florida Institute of Technology:

Completion of the procurement of all parts for the next FT GEM detector was delayed. Reasons were the need for a substantial redesign of the vias in the 1-meter-long zigzag readout foil, delays in production of precision laminated plywood templates for carbon fiber frames, and the need of our departing post-doc to secure a new position.

INFN Trieste:

N/A

Stony Brook University:

The final upgrade of the evaporator unit has not happened due to delayed purchase options from appropriate equipment providers.
The design of a snowflake readout pad had been postponed due to the support activity of the TPCC effort of BNL.

University of Virginia:

1. The design of the overall mechanical structure of large EIC GEM chamber (prototype II) including the GEM support frames has been put on hold during this term due to lack of funding. Though the 4 GEM foils (common design) have already been delivered to our group at UVa, we have decided to postpone the electrical tests on the foils since these tests are meaningful only when one is ready for the assembly of the chamber. The design of the U-V strips readout board is also almost completed and with the successful test of the zebra connection on a small prototype, we are ready to finalize the design and launch the part production and the assembly of the chamber.
2. The assembly of 10 cm × 10 cm GEM prototype with the small U-V strip readout and the zebra connection scheme was a little bit delayed because by late delivery of the parts from CERN. However, we have completed the assembly and perform preliminary tests with cosmic, which yield some very promising results. We are also in the process of migrating the APV25-SRS based readout system in our detector R&D lab, from a stand-alone DAQ software to the DAQ compatible with JLab CODA framework that was developed for the PRad experiment at JLab last spring 2016. This has delayed the full analysis of the cosmic data needed to complete the characterization of the U-V strip readout and zebra connection.
3. We were not able to make much progress with the Chromium GEMs (Cr-GEMs) aging study because of bad quality foils that we received from CERN. We suspect that the Cr layer was removed during the etching process of the Cu. The small prototype that we put together with these foils did not work and we are waiting for new foils from CERN to resume the aging study.

Yale University:

We are still waiting for next production and delivery step from CERN micropattern detector workshop to finish all needed tests for 2-GEMs + MMG setup with R-protection MMG read-out.
We have not a chance to test negative and fast HV switches in a combination with pico-amperemeters to measure the crucial parameter: how fast positive ions can be collected in such multi-gate structure to compare with simulation results and measure how much dead time is required.

Future

What is planned for the next funding cycle and beyond? How, if at all, is this planning different from the original plan?

Brookhaven National Lab

1. We plan to publish our results from the beam test of the TPC/Cherenkov prototype detector in the IEEE Transactions on Nuclear Science. We hope to have the final manuscript completed and submit it for publication in early 2017.
2. We expect to receive the new chevron readout board back from the manufacturer by early February 2017. We will then assemble it together with a quadruple GEM detector and measure its properties using our new high power X-ray scanner. We will then assemble it together with our TPC prototype detector and measure cosmic rays in our lab. However, our current cosmic ray telescope consists only of simple scintillation counters and does not provide any tracking information. We would, therefore, like to purchase a new set of GEM detectors from CERN with COMPASS readout boards and incorporate them into our cosmic ray setup. This would also include acquiring a new SRS readout crate, FEC cards and APV25 cards for their readout, since our current SRS system, which was one of the first early prototypes produced at CERN, does not allow for expanding the readout. It would also be extremely beneficial if we could test our TPC setup at the NASA Space Radiation Lab (NSRL) at BNL, which can provide excellent quality beams of 1-2 GeV protons that would be ideal for testing this type of detector. **It is known that it is possible to test such detectors at this facility and that it only has to be made available to us at no charge.** Being able to test small prototypes and their associated electronics at this facility would be an enormous benefit towards building and testing a full-scale prototype TPC for future use at RHIC or EIC.
3. We will finish the assembly of our new high power, large area X-ray scanner and use it to scan our new chevron readout board. If funding becomes available, we will also have other chevron patterns made and measure those in the new scanner. The scanner will be fully automated and will provide data at a much higher rate than our existing scanner, and we plan to make it available to other members of our collaboration.
4. We will continue our studies of various gas mixtures for a TPC, focusing mainly on high ion mobility gas mixtures containing neon. We would also like to study the use of GEMs with a larger hole to hole spacing, such as are being employed by the ALICE Collaboration, in order to reduce ion feedback, but we need additional funding to purchase them.
5. We would like to study new types of readout electronics, such as the system based on the SAMPA chip that is being developed by ALICE, but we do not plan to get directly involved with any electronic development due to lack of resources.

Florida Institute of Technology:

Our main goal for the next six months is to complete production of all components for the new one-meter-long FT GEM detector with zigzag readout, assemble it, and put it through a battery of quality control tests modeled on the QC for the large GEM detectors of the CMS forward muon upgrade.
In parallel, we are finalizing a publication on the results of the X-ray studies that are reported here.

INFN Trieste:

Further development of hybrid MPGDs for single photon detection synergic to TPC read-out sensors; three-year activity.

The concept of the hybrid MPGD detector of single photons has been developed in an eight-year R&D program; the reference figures for the present optimization are the requirement for the upgrade of the gaseous RICH counter of the COMPASS experiment at CERN SPS. The resulting detectors, installed during Spring 2016, have been commissioned during the 2016 COMPASS data taking. The detector architecture consists of three multiplication stages: two THick GEMs (THGEM) layers, the first one coated with a CsI film and acting as a photocathode, followed by a MicroMegas (MM) multiplication stage. The two THGEMs are staggered: this configuration is beneficial both to reduce the Ion BackFlow (IBF) and to increase the maximum gain at which the detector can be operated exhibiting full electrical stability. These photon detectors can operate at gains of at least 5×10^4 and exhibit an IBF rate lower than 5%. The gas mixtures used are by Ar and CH_4, with a rich methane fraction in order to maximize the photoelectron extraction.

An original element of the hybrid MPGD photon detector is the approach to a resistive MM by discrete elements, which has been triggered by the resistive MM developed for the ATLAS experiment at CERN LHC [The ATLAS Collaboration, "Technical Design Report for the New Small Wheel," CERN-LHCC-2013-006 / ATLAS-TDR-020, June 2013], but presents substantial differences. The anode elements (pads) facing the micromesh are individually equipped with large-value resistors and the HV is provided, via these resistors, to the anode electrodes, while the micromesh is grounded. The second set of electrodes (pads parallel to the first ones) are embedded in the anode PCB: the signal is transferred by capacitive coupling to these electrodes, which are connected to the front-end read-out electronics. The advantages of the design shortly described above are several:

- As in ATLAS resistive MM, applying the HV to the anode instead of to the MM cathode results in larger amplitude signals;
- In case of local defects of the MM, a single electrode can be isolated resulting in a dead area as large as the electrode itself, while the large majority of the detector is still active;
- No resistive coating is present inside the detector volume;
- The absence of a resistive layer on top of the anode electrodes is limiting the degradation of the dE/dx information in the collected signals.

The hybrid detector concept can be further improved in order to match the requirements of high momentum hadron identification at EIC; this challenging task requires:

i. Limited radiator length of the order of 1 m: here one of the most promising approaches is the window-less RICH concept [M. Blatnik et al., IEEE Transaction on Nuclear Science 62 (2015) 3256];
ii. Fine space granularity to cope with the modest lever arm related to the radiator length;
iii. Control of the IBF rate in order to guarantee stable detector performance over time;
iv. Further improvement in the engineering aspects in order to simplify the construction and control the costs;
v. The comparison between hybrid detectors where THGEMs or GEMS in view of an overall optimization of the detector principle.

The R&D program proposed here is meant to match the requirements listed above. It spans three years of activity and it includes five tasks:
1. test of novel materials for THGEM substrate to simplify the detector construction, increase the yield of valid large-size THGEMs and, thus, control the detector costs (related to requirement iv);
2. the development of resistive MM by discrete elements with miniaturized pad size (present size: 8 x 8 mm2) in order to obtain finer space resolution (related to requirement ii);
3. comparison of THGEM vs GEM photocathodes in order to select the best architecture for the photon detectors of the EIC RICH (related to requirement v);
4. further studies in order to enhance the IFB suppression in hybrid MPGDs (related to requirement iii);
5. operation of hybrid MPGDs (THGEMs + MM) in fluorocarbon-rich gas mixtures (related to requirement i).

It is relevant to underline that the further development of the hybrid detector concept, in particular with finer space resolution and low IBF rate is synergic to another sector of great relevance for the future experiments at EIC, namely the read-out sensors for the TPC. A hybrid MPGD approach to TPC read-out has already been proposed making use of traditional non-resistive MMs [A. Aiola et al., "Combination of two Gas Electron Multipliers and a Micromegas as gain elements for a time projection chamber", http://arxiv.org/abs/1603.08473, submitted to Nucl. Instr. Meth. A]; our approach to resistive MM can offer a detector which exhibits robust electrical stability while preserving a good dE/dx resolution.

In particular, the activity foreseen for the next funding cycle consists in (1) test of novel materials for THGEM substrate, a task expected to be completed within the first year of activity and (2) the development of resistive MM by discrete elements with miniaturized pad size, a task that will be performed over two years.

Stony Brook University:

The finalization of redesigning the evaporator for producing large mirrors is expected to be performed in the Spring term of 2017. After receiving the equipment it will be installed and tested. We will be learning to properly operate the equipment and then provide a large surface equipped with smaller mirror blanks at each corner and in the center. The samples will then be evaluated with the VUV spectrometer from BNL. This should represent a good measure of the properties of a large mirror evaporation.

University of Virginia:

1.R&D on Chromium GEM

We plan to perform the long-term stability study of the Cr-GEM chamber. We will first assemble a prototype with the remaining two good quality Cr-GEMs from the first batch with one standard GEM foil and test the chamber with the x-ray source in moderate background rate environment. This test will go on until we receive a new batch from CERN to replace the standard GEM foil by a Cr-GEM. We anticipate this test campaign to last a couple of months for the results to be meaningful.

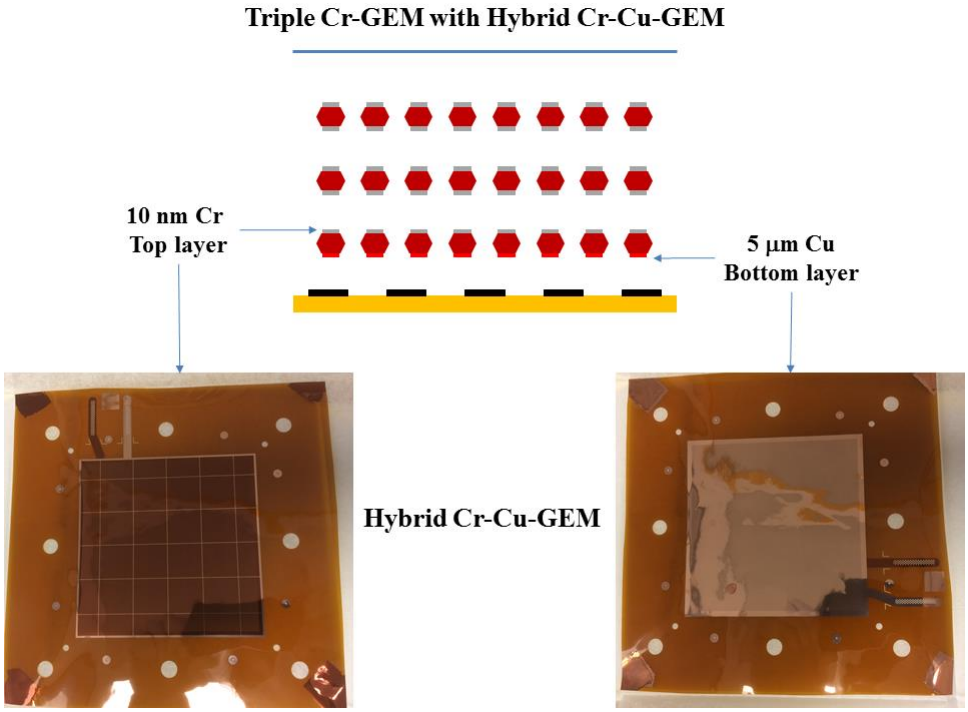

Figure 27 Figure 6: Top: Sketch of a triple-GEM detector with Cr-GEM foils and one hybrid Cr-Cu-GEM foil. Bottom: Pictures of the hybrid Cr-Cu-GEM with the top side with Chromium electrode (left) and the bottom side with the Copper electrode (right).

As already reported, the degradation that we observed with the exposure to the high-intensity x-ray source affected only the bottom electrode of the third Cr-GEM foil. We suspect that mini discharges triggered by the high concentration of charges at the bottom electrode are responsible for the "evaporation" of the Cr layer. The discharges are quickly and effectively quenched by the evaporation of the Cr layer which in turn would prevent the development into a larger spark and the propagation to the top side of the GEM and to the other GEM foils. After the aging test is completed, we will test this hypothesis in a triple-GEM chamber with Cr-GEM used as the two first foils and a hybrid Cr-Cu-GEM for the third application foil where the Cu layer is removed only from one side (top side) of the GEM and the Cu electrode left on the bottom side as illustrated in Figure 27.

Additionally, we are also looking at the possibility to inspect the damaged Cr-GEM foil from the first prototype and the bad foils of the second under SEM microscopy to acquire a high-resolution picture of the aging process and the radiation damage. The idea is to investigate the cause of the evaporation of Cr layer. Several studies in the literature have shown that under extreme high rate environment, the polyimide layer of

a standard GEM foil (with 5 μm Cu as an electrode) is etched out inside the holes. Various groups are studying this effect. The etching of the Kapton layer would not explain the evaporation of the Cr layer in the case of Cr-GEM chamber but can provide additional information about the underlying cause of the Cr disappearance. An inspection under SEM microscope of the cross-section damage Cr-GEM and a comparison with the good Cr-GEM will provide meaningful information on the shape of the holes in both cases and whether the polyimide was etched out during the exposure of the foils to the high rate x-ray source. To examine the shape of the holes of the Cr-GEM foil, one needs to find a safe way to cut the GEM foil to expose its cross section. This represents a challenge since a simple cut of the foil will destroy the information on the geometry of the holes. We will contact the Advanced Microscopic Facility at UVa to discuss different techniques to safely cut the Cr-GEM foil and prepare the samples to perform the SEM measurement.

2. **Assembly and characterization the large EIC GEM prototype II**

We would like to assemble the full-size EIC GEM prototype II. For this, we must finalize the drawings of the U-V strip readout board and the zebra connection after we complete the analysis of the cosmic data to fully validate the concept with the small prototype. We will work on the design of GEM support frames and the mechanical components of the full chamber. We expect to start the production of the U-V strips readout board at CERN and the GEM support frames soon after the funds become available and will be ready for the assembly of the chamber and the characterization with Cosmic and X-ray as well as in test beam that we anticipate will likely be scheduled for the following funding cycle of July – December 2017.

Yale University:

Our plan is to finish all R&D activities mentioned above and prepare at least 2 publications.

What are critical issues?

Brookhaven National Lab

Our main critical issue now is a lack of funding. The development of the new chevron readout board expended essentially all our existing R&D funds and we now have very little funds left to operate with. **It will, therefore, be crucial for us to obtain additional new funding during the next funding cycle for us to continue our R&D efforts on this project**.

Florida Institute of Technology:

The departure of our post-doc Aiwu Zhang will severely slow down future progress. There is zero new funding in 2017 to help complete this project.

INFN Trieste:

N/A

Stony Brook University:

The installation of the ordered equipment and working mode for the vacuum evaporator is the critical issue to finalize the evaporation of a large sized mirror.

University of Virginia:

As mentioned in the previous report, we have developed a common GEM foil design for EIC GEM chambers together with our colleagues from Florida Tech and Temple U. The UVa group had already received 4 common GEM foils. We have also nearly completed the design of the new U-V strips readout board for which we anticipate some significant improvements. The time scale for finalizing the design and/or the fabrication of the various components such as the U-V strips readout board or the GEM support frames, that are critical for the assembly of the prototype is estimated to be roughly one funding cycle. We expect the timeline for the assembly of the chamber and the full characterization in our detector lab and in test beam to be about an additional 6 months' cycle. If we are to complete the R&D program at UVa by December 2017, it is critical that we obtain the funding for the parts production in a timely manner.

Yale University:

None.

Additional information:

N/A

Manpower

Brookhaven National Lab

This work is being carried out by members of the BNL Physics Department. It includes one Senior Scientist (0.2 FTE), one Physics Associate (1.0 FTE), one Assistant Physicist (0.1 FTE) and one Technician (0.3 FTE). All personnel is paid by the BNL Physics Department.

Florida Institute of Technology:

Marcus Hohlmann, P.I., 0.25 FTE, not funded under this R&D program.
Aiwu Zhang, post-doc, 1 FTE, fully funded under this R&D program, located at Florida Tech, supervised by M. Hohlmann. Aiwu's funding and participation in the project were terminated as of December 2016.
Matthew Bomberger, undergraduate student, not funded under this R&D program.

INFN Trieste:

Trieste personnel involved in the project during the coming year:
C. Chatterjee (Trieste University and INFN, Ph.D. student)
S. Dalla Torre (INFN, Staff)
S. Dasgupta (INFN, postdoc)
G. Hamar (INFN, postdoc)
S. Levorato (INFN, Staff)
F. Tessarotto (INFN, Staff)
1 new postdoc specifically enrolled for this R&D (INFN); the position will be open in Spring and the postdoc will work under the supervision of S. Levorato and F. Tessarotto. Globally the dedicated manpower will be equivalent to 2 FTE. The contribution of technical personnel from INFN-Trieste is also foreseen according to needs.

Stony Brook University:

None of the labor at SBU is funded by EIC R&D. The workforce is
K. Dehmelt, Research Scientist, 0.4 FTE, T. K. Hemmick, Professor, 0.1 FTE, N. Nguyen, Undergraduate student, 0.25 FTE

University of Virginia:

None of the labor at UVa is funded by EIC R&D. The workforce is listed below (in % FTE):

N. Liyanage	Professor	10%
K. Gnanvo	Research Scientist	40%
Siyu Jian	Graduate Student	5%

Yale University:

None of the labor at Yale is funded by EIC R&D. The workforce is listed below.

R. Majka	Senior Research Scientist and Scholar	10%
N. Smirnov	Research Scientist and Scholar	50%

External Funding

Describe what external funding was obtained, if any. The report must clarify what has been accomplished with the EIC R&D funds and what came as a contribution from potential collaborators.

Brookhaven National Lab

Aside from supporting the personnel involved in this effort by the BNL Physics Department, we are not receiving any other funding from any other source. It should be noted that the sPHENIX Collaboration is developing a TPC for the sPHENIX experiment but our R&D on this project is not being supported by this effort.

Florida Institute of Technology:

None.

INFN Trieste:

A request for financial support from INFN has been placed for 2017: the outcome is expected by March 2017.

Stony Brook University:

There is no external funding for this R&D effort.

University of Virginia:

UVa has DOE basic research grant from Medium Energy Physics. The R&D work on Cr-GEM is funded with the research grant.
The group also has DOE grants through JLab for the construction of the SBS GEM.

Yale University:

None.

Publications

Brookhaven National Lab

1. Manuscript in preparation: “First Results from a Prototype Combination TPC Cherenkov Detector with GEM Readout”, to be submitted to the IEEE Transaction on Nuclear Science in early 2017, see Stony Brook publications
2. Oral presentation at the IEEE NSS/MIC conference in Strasbourg, France in November 2016 on the TPC/Cherenkov hybrid detector, see Stony Brook publications
3. B. Azmoun et al., “A Study of a Mini-drift GEM Tracking Detector “, IEEE Trans. Nucl. Sci. Vol. 63, No.3, June 2016, pp. 1768-1776.
4. C. Woody et. al.: “A Prototype Combination TPC Cherenkov Detector with GEM Readout for Tracking and Particle Identification and its Potential Use at an Electron Ion Collider”, Conference Proceedings of the 2015 Micropattern Gas Detector Conference, Trieste, Italy, October 12-15, 2015.
5. M.L. Purschke, “Test Beam Study of a Short Drift GEM Tracking Detector” Conference Record Proceedings of the 2013 IEEE Nuclear Science Symposium and Medical Imaging Conference, October 27-Nov 2, 2013, Seoul, Korea

Florida Institute of Technology:

1. A. Zhang and M. Hohlmann, "Accuracy of the geometric-mean method for determining spatial resolutions of tracking detectors in the presence of multiple Coulomb scattering," JINST 11 P06012 (2016), June 21, 2016; preprint version arXiv:1604.06130, Apr 20, 2016.
2. A. Zhang, et al., "Performance of a large-area GEM Detector read out with wide radial zigzag strips," Nucl. Inst. Meth. A 811 (2016) 30-41, online version at ScienceDirect (18 Dec 2015); preprint version arXiv:1508.07046, Aug 2015.
3. A. Zhang, V. Bhopatkar, M. Hohlmann, et al., "R&D on GEM Detectors for Forward Tracking at a Future Electron-Ion Collider", Proc. of IEEE Nuclear Science Symposium 2015, San Diego, CA; arXiv:1511.07913, Nov 24, 2015.
4. A. Zhang, et al., “Study of non-linear response of a GEM detector read out with radial zigzag strips,” in preparation for submission to NIM A and presented as a poster at the 2016 IEEE NSS, Strasbourg, France.
5. M. Bomberger, et al., “Mechanical design and stress analysis of a large-area gas electron multiplier,” in preparation for submission to Journal of Mechanical Design (JMD). This work has also been submitted to the Florida Academy of Sciences (FAS) annual meeting in 2017.

INFN Trieste:

N/A

Stony Brook University:

1. M. Blatnik et al., "Performance of a Quintuple-GEM Based RICH Detector Prototype", IEEE TRANSACTIONS ON NUCLEAR SCIENCE, VOL. 62, NO. 6, DECEMBER 2015.
2. M. Blatnik et al., "Performance of a Quintuple-GEM Based RICH Detector Prototype", Nuclear Science Symposium Conference Record, 2015, IEEE
3. Manuscript in preparation: "First Results from a Prototype Combination TPC Cherenkov Detector with GEM Readout", to be submitted to the IEEE Transaction on Nuclear Science in early 2017, see BNL publications
4. Proceedings in preparation: "First Results from a Prototype Combination TPC Cherenkov Detector with GEM Readout", for the IEEE NSS/MIC 2016 in Strasbourg, see BNL publications

University of Virginia:

1. K. Gnanvo, et al., "Large Size GEM for Super Bigbite Spectrometer (SBS) Polarimeter for Hall A 12 GeV program at JLab", Nucl. Inst. and Meth. A782, 77-86 (2015). *DOI: 10.1016/j.nima.2015.02.017*
2. K. Gnanvo et al., "Performance in Test Beam of a Large-area and Light-weight GEM detector with 2D Stereo-Angle (U-V) Strip Readout", Nucl. Inst. and Meth. A808 (2016), pp. 83-92. *DOI: 10.1016/j.nima.2015.11.071*

Yale University:

1. S. Aiola et al., "Combination of two Gas Electron Multipliers and a Micromegas as gain elements for a time projection chamber", Nucl. Inst. and Meth. A834 (2016) 149-157.